Colloids and Surfaces B: Biointerfaces 185 (2020) 110581

Contents lists available at ScienceDirect

Colloids and Surfaces B: Biointerfaces

journal homepage: www.elsevier.com/locate/colsurfb

Non-proteinogenic amino acid based supramolecular hydrogel material for enhanced cell proliferation

Jaini Flora Arokianathan[a,b], Koduvayur A Ramya[c], Asuma Janeena[d], Abhijit P. Deshpande[c], Niraikulam Ayyadurai[d], Ambrose Leemarose[b], Ganesh Shanmugam[a,e,*]

[a] Organic & Bioorganic Chemistry Laboratory, CSIR-Central Leather Research Institute, Adyar, Chennai-600 020, India
[b] Department of Chemistry, Holy Cross College (Autonomous), Tiruchirapalli, 620 002, India
[c] Department of Chemical Engineering, Indian Institute of Technology Madras, Chennai 600036, India
[d] Biochemistry & Biotechnology Laboratory, CSIR-Central Leather Research Institute, Adyar, Chennai-600020, India
[e] Academy of Scientific and Innovative Research (AcSIR), CSIR-CLRI Campus, Adyar, Chennai-600 020, India

ARTICLE INFO

Keywords:
Hydrogel
Non-proteinogenic
Cell viability
Drug delivery
2,3-diamino propionic acid

ABSTRACT

Supramolecular gel material built from low-molecular-weight (LMW) gelators finds potential applications in various fields, especially in drug delivery, cell encapsulation and delivery, and tissue engineering. The majority of the LMW gelators in these applications are based on functionalized peptides/amino acids consisting of proteinogenic amino acids which are proteolytically unstable. Herein, we have developed a new LMW gelator containing non-proteinogenic amino acid namely 2,3-diaminopropionic acid (Dap), a key precursor in the synthesis of many antibiotics namely viomycin and capreomycin, by functionalizing with fluorenylmethoxycarbonyl at both amino terminals of Dap [Fm-Dap(Fm)]. Hydrogelation test at different pH indicates that Fm-Dap(Fm) can form a hydrogel in a wide range of pH (4.9 to 9.1) with minimum hydrogelation concentration depends on the pH. The mechanical strength and thermal stability of the Fm-Dap(Fm) hydrogel material are found to decrease with increasing pH (acidic > neural/physiological > basic). The thermal stability of Fm-Dap (Fm) hydrogels is pH-dependent and elicits high stability at acidic pH. Also, Fm-Dap(Fm) hydrogels exhibit strong thixotropic property where regelation (self-healing) occurs upon release of stress. Morphological analysis indicates the formation of fibrils, which are entangled to form three dimensional network structures. Several spectroscopic measurements provided evidence for the self-assembly of Fm-Dap(Fm) molecules through intermolecular aromatic π-π stacking and hydrogen bonding interactions during hydrogelation. Interestingly, Fm-Dap (Fm) not only exhibits hydrogel formation but also shows cell viability and enhanced cell proliferation at physiological pH (7.4). Further, Fm-Dap(Fm) forms a hydrogel upon co-incubation with vitamin B_{12} and also exhibits release of vitamin B_{12} over a period. The current study thus demonstrates the development of a new hydrogel material, based on LMW gelator containing the non-proteinogenic amino acid, which can elicit cell viability, enhanced cell proliferation, drug encapsulation, and drug release properties. Hence, Fm-Dap(Fm) hydrogel could be an ideal material for biomedical applications, especially in tissue engineering and drug delivery.

1. Introduction

Supramolecular gel materials continue to attract many researchers due to their potential applications in diverse fields such as drug delivery, cell culturing, tumor therapy, sensing, storage, encapsulation, electronic materials, removal of pollutants from wastewater, and others [1–10]. These gel materials are constructed using low molecular weight (LMW) compound (referred to as gelator), which are self-assembled through various non-covalent interactions, including aromatic π-π stacking, hydrogen bonding, hydrophobic, ionic and van der Waals interactions to form three dimensional network structure. These network structures can trap water or organic solvents to form hydro and organogels, respectively. Supramolecular gel materials derived from LMW compounds offer significant advantages mainly stimuli-responsive with pH, temperature, chemical or photochemical reactions, ionic strength, and so on [5,11–13] while a simple swelling usually confers a polymeric gel. Among the LMW gelators, amino acid and peptide-based supramolecular gel materials gain more attention due to

* Corresponding author at: Organic & Bioorganic Chemistry Laboratory, CSIR-Central Leather Research Institute, Adyar, Chennai-600 020, India.
E-mail addresses: ganeshclri@gmail.com, ganesh@clri.res.in (G. Shanmugam).

https://doi.org/10.1016/j.colsurfb.2019.110581
Received 3 July 2019; Received in revised form 11 October 2019; Accepted 13 October 2019
Available online 16 October 2019
0927-7765/ © 2019 Elsevier B.V. All rights reserved.

biocompatibility and biodegradability.

While gel materials find applications in various fields, the use of supramolecular hydrogel is profoundly witnessed in tissue engineering and drug release [14–16]. Many of the supramolecular hydrogels used for these applications are often constructed using smaller peptides which are conjugated with aromatic groups including Fluorenylmethoxycarbonyl (Fmoc) [1,17], naphthyls [18], and substituted benzyl [19] at the amino group of N-terminal amino acid in the peptide. Among these conjugating agents, Fmoc is the choice for the researchers due to ease synthesis [20] and commercial availability of Fmoc-amino acids. Vegners et al. reported the first Fmoc-based dipeptide gelator which shows the formation of hydrogel under the select experimental condition and used as a carrier for the antigen [21]. Followed by this finding, several N-terminal protected short peptides have been constructed by various research groups and contributed significantly to the development of peptide-based hydrogel materials [19,22–26]. However, these gelators are constructed using mostly natural, proteinous amino acids. Therefore, there is a requirement to develop peptide or amino acid-based supramolecular gelator containing non-proteinogenic amino acids, which could be an alternate approach to overcome proteolysis. The choice of the non-proteinogenic amino acid is based on the previous reports where several congener proteins are biosynthesized and explored in biomedical, therapeutic, and cell biology applications [27]. Adding non-proteinogenicamino acid will expand the scope of research in supramolecular gels towards therapeutic applications.

Although the substitution of non-proteinogenicamino acid successfully utilized in ribosomal protein synthesis, amino acid-based LMW gelators comprising non-proteinogenic amino acids are less explored. Hereby we have developed a new amino acid-based LMW gelator containing non-proteinogenic amino acid namely 2,3-diaminopropionic acid (Dap) by functionalizing both amino groups with fluorenylmethoxycarbonyl [Fm-Dap(Fm)]. Dap is a key precursor in the synthesis of many antibiotics, specifically viomycin and capreomycin [28,29]. Further, Dap-based compounds have been successfully used as scavengers of α-oxoaldehydes [30], which are inherently toxic as well as serving as precursors for glycation end-products. Furthermore, the incorporation of Dap in cationic amphipathic peptides produces a system which efficiently used for robust gene-delivery [31]. Meanwhile, it has been well established that fluorenyl moiety in Fmoc- group has a strong ability to bring intermolecular aromatic π-π stacking interactions which facilitate supramolecular self-assembly and thereby induce gelation [4,32]. Further, Fm-Dap(Fm) possesses not only two fluorenyl moieties at both the end of the molecule but also has two amide groups which may provide necessary intermolecular interactions that can facilitate the self-assembly process and thereby gelation.

2. Experimental section

2.1. Materials

Fm-Dap(Fm) (74391) and vitamin B_{12} (V2876) were purchased from Sigma-Aldrich (India).

2.2. Hydrogel preparation

A stock solution of Fm-Dap(Fm) was prepared in DMSO at a concentration of 400 mM. For different pH, 50 mM of sodium acetate, 50 mM sodium phosphate, and 50 mM of sodium carbonate buffers were prepared for pH 4.9, 7.4, and 9.1, respectively. Hydrogels were formed in a glass vial by diluting the stock solution of Fm-Dap(Fm) with respective buffer solutions. For finding minimum gelation concentration, an appropriate volume of stock solution of Fm-Dap(Fm) was diluted with an appropriate volume of DMSO and buffer solutions to obtain a different concentration of Fm-Dap(Fm). The final volume of DMSO in each mixture was maintained at 3% (v/v). The final mixture was kept at ambient temperature for gel formation. The diameter of the vails in which hydrogelation test conducted was 15 mm. All hydrogels were repeated several times for biophysical experiments (vide infra) and the formation hydrogel was reproducible. Further, all biophysical experiments were repeated at least twice, and the data were consistent with each other.

2.3. Thermal stability analysis

Fm-Dap(Fm) hydrogels at different pH were prepared in glass vials as described earlier. Hydrogels were transferred to IKA RCT basic dry block heater, and the temperature was increased to the desired temperature. The sample vial was immediately returned to the dry block heater after capturing the image at a selected temperature.

2.4. SEM analysis

Phenom-pro scanning electron microscope was used to record SEM images. The Fm-Dap(Fm) hydrogels were coated on the glass coverslip and air-dried overnight. Gold was spattered on the dried samples before scanning for the picture.

2.5. AFM measurements

XE-70 park system (South Korea) was used to capture AFM images of air-dried Fm-Dap(Fm) hydrogels on a glass plate. A semi-contact mode was used. A cantilever was set vibrating in the z-direction with a resonance frequency of 330 kHz.

2.6. TEM measurements

A small quanity of Fm-Dap(Fm) hydrogels were dried on copper grids (Cu-300HD), and TEM images were captured using tabletop Delong Instruments (LVEM5).

2.7. Rheological measurements

All rheological measurements were performed on an Anton Paar MCR-301 rheometer. An oscillatory mode with a 25 mm parallel plate geometry was used. Fm-Dap(Fm) hydrogels were prepared in a glass vial and shifted to the lower plate (1 mm gap). Strain sweep, frequency sweep, thixotropic cycle, and temperature sweep experiments were performed as reported previously [33].

2.8. Fluorescence measurements

A Carry (eclipse) fluorescence spectrometer was used for all fluorescence experiments at 25 °C. Fluorescence emission spectra (300–550 nm) were collected for Fm-Dap(Fm) in both the hydrogel and solution form at different pH. A low concentration of 0.01 wt% in the corresponding buffer solutions was used to represent the solution form. Hydrogels were formed directly in a 1 cm quartz cell by following the method reported *vide supra*. The fluorescence was excited at 285 nm with a setting of an excitation and emission slit width of 2.5 nm.

2.9. Circular dichroism measurements

A JASCO-715 spectropolarimeter was used to measure all CD measurements. Hydrogels were directly formed in a 0.1 cm rectangular quartz cell. The stock solution of Fm-Dap(Fm) was diluted with methanol to represent a solution form. Owing to high HT at the minimum gelation concentration of Fm-Dap(Fm), the CD spectra were measured between 350 and 270 nm with a scan speed of 100 nm/min. For baseline corrections, each CD spectrum was subtracted from the corresponding buffer/methanol solutions.

2.10. Fourier transform infrared measurements

A JASCO-4700 spectrometer was used to collect all the FTIR spectra in ATR mode. Air dried samples of hydrogels were placed on the ATR crystal, and the spectrum was recorded at 8 cm^{-1} resolution with a total of 64 scans. For solution measurements, Fm-Dap(Fm) was dissolved in DMSO-d_6 (30 mg/ml). A fixed path length cell (50 μm) containing CaF_2 windows was used. FTIR spectrum of neat DMSO-d_6 was subtracted from the sample spectrum to obtain a baseline. The total number of scans for solution FTIR was 512.

2.11. NMR measurements

Temperature-dependent ^{1}H NMR spectra of Fm-Dap(Fm) hydrogels were measured on Bruker (400 MHz) spectrometer with water presaturation pulse program. Fm-Dap(Fm) hydrogels were prepared by diluting its stock solution (prepared in DMSO-d_6) with 50 mM buffers (prepared in D_2O) with different pH. The final concentrations of the hydrogel were 0.3, 1.3 and 1.3 wt% at pH 4.9, 7.4, and 9.1, respectively, and DMSO-d_6 was 3% (v/v).

2.12. UV–vis measurements

UV-visible spectra of Fm-Dap(Fm) hydrogels at 0.3 wt% (pH 4.9), 1.3 wt% (pH 7.4) and 1.3 wt% (pH 9.1) were recorded on a Jasco (V-730) spectrophotometer at 25 °C. A quartz cell with a pathlength of 1.0 mm was used.

2.13. Proteolytic stability studies

The Fm-Dap(Fm) hydrogel (pH 7.4) was formed in two vials equally (1 ml) by following the method as described previously. After incubation of these hydrogels overnight at room temperature, 1 ml of phosphate buffer (control) and 1 ml of phosphate buffer containing proteinase K (0.2 mg/ml) (test) was added on the top of the hydrogels. After 48 h incubation at room temperature, the absorbance of the added buffer solution was measured at 303 nm, corresponding to fluorenyl moiety, using UV–vis spectrophotometer. The digital images of both hydrogels (control and test) were also captured immediately and after 48 h incubation with proteinase K.

2.14. Drug release studies

Fm-Dap(Fm) hydrogel (pH 7.4) co-assembled with vitamin B_{12} was prepared by diluting the stock solution of Fm-Dap(Fm) with a phosphate buffer solution containing vitamin B_{12} (92 μM). The concentration of Fm-Dap(Fm) was 1.5 wt%. After hydrogel formation (overnight), 1 ml of phosphate buffer (pH 7.4) was added on the top of Fm-Dap(Fm)-vitamin B_{12} hydrogel. At different time intervals, the top buffer solution was transferred to UV cuvette to read the absorbance at 525 nm (corresponding to vitamin B_{12}), and the solution was returned to the same place immediately after the measurement. The absorbance of vitamin B_{12} at a concentration of 92 μM (total concentration in 1 ml of hydrogel) was taken as 100%.

2.15. pXRD studies

Powder XRD was measured for the air-dried hydrogels of Fm-Dap (Fm) using a Rigaku, MiniFlex (II) X-ray diffractometer. The instrument was operated Cu (0.154 nm) radiation, and power settings were 30 kV and 15 mA. The measurements were carried out between 5 and 80° with a scan rate of 2°/min.

2.16. Fluorescence microscopic studies

The 3T3 cells were cultured on different concentration of Fm-Dap (Fm) hydrogel coated in a 12 well plate and kept overnight at 37 °C with the supplementation of 5% CO_2. Subsequently, cells were washed with 1X PBS. Calcein AM/ethidium bromide (Calcein AM/EB) was used as the fluorescent dye to determine the rates of cell proliferation and apoptosis. Dual fluorescent staining solution (5 μl) containing 10X Calcein AM and 100 μg/ml EB (AO/EB, Sigma, St. Louis, MO) was added to each well. The morphology of apoptotic cells was examined using a fluorescence microscope (Leica DMi8, Germany). The fluorescence image of Fm-Dap(Fm) hydrogel treated 3T3 cells were obtained in 10X magnification. For calcein AM, the excitation and emission filters were at 495 nm (FITC filter) and 519 nm, respectively. The exposure time was 333.544 ms. For EB, the excitation and emission filters were at 552 nm (rhodamine filter) and 598 nm, respectively. The exposure time was 183.044 ms.

2.17. Cell viability and proliferation study

Cell viability of Fm-Dap(Fm) hydrogel was tested with fibroblast (3T3) cell and the detailed procedure is given in the supporting information (page 21).

2.18. Flow cytometry studies

To explore cell proliferation, PCNA, and Ki-67 markers were used for flow cytometry analysis. A detailed experimental procedure is given in supporting information (page 21).

2.19. Gene expression studies using real time-PCR

A detailed experimental procedure on RNA isolation, complementary DNA synthesis, and real-time PCR is presented in supporting information (page 22).

3. Results and discussion

3.1. Hydrogelation studies

Hydrogelation of Fm-Dap(Fm) was induced by the solvent dilution technique while the formation of hydrogel was confirmed by conventional vial inversion method. Accordingly, Fm-Dap(Fm) was dissolved in DMSO, followed by the addition of a buffer solution with different pH. Initially, hydrogelation was tested at three different pH representing the acidic (4.9), neutral/physiological (7.4), and basic (9.1). It was observed that the solution mixture was transformed into a milky solution after addition of buffers. The solutions became transparent in a short period, and the mixture was kept at room temperature for gel formation. As expected, the minimum concentration and minimum time required for the gelator to immobilize the total volume of the solution was found to be pH dependent. As a representative, Fm-Dap(Fm) hydrogels formed at different pH in the vial inverted position is presented in Fig. 1. At acidic pH (4.9), Fm-Dap(Fm) displays MHGC as low as 0.3 wt% while below this concentration the solution was clear and remained the same with time (Fig. 1 and Fig. S1). The minimum gelation time was less than 30 min. While increasing the pH, the MHGC was increased to 1.0 and 1.3 wt% at pH 7.4 (Fig. 1 and Fig. S2) and 9.1 (Fig. 1 and Fig. S3), respectively, and also the gelation time was increased (overnight) at both the pHs. Although Fm-Dap(Fm) displayed viscous/gel nature at 1.0 wt% in pH 9.1, the corresponding hydrogel was not self-supportive upon vial inversion under similar condition compared to other pHs (Fig. S3). Acidic pH was extended to 3.8 to understand the broad range of pH at which Fm-Dap(Fm) induce hydrogels. However, there was no gelation at pH 3.8. Instead, Fm-Dap (Fm) exhibited white turbid solution upon addition of buffer, which remains the same with time (Fig. S4). We did not extend the pH above 9.1 due to the instability of Fmoc protection with an amino group at higher basic pH. The current hydrogelation study thus concludes that

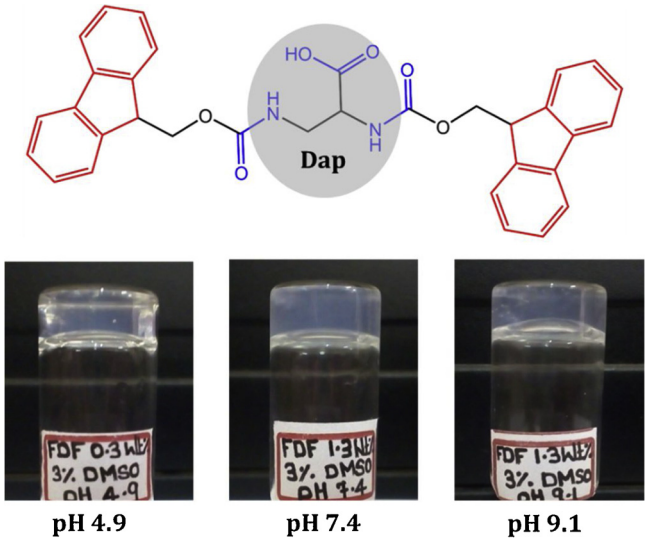

Fig. 1. (Top) Chemical structure of Fm-Dap(Fm) gelator. The red and blue indicate the sites for the intermolecular aromatic π-π stacking and hydrogen bonding interactions, respectively. (Bottom) Representative digital images of Fm-Dap(Fm) hydrogel (vial inverted) formed at different pH. The concentrations of hydrogels were 0.3, 1.3, and 1.3 wt% at pH 4.9, 7.4, and 9.1, respectively.

Fm-Dap(Fm) has gelation ability in a broad range of pH (4.9–9.1). It was also observed that Fm-Dap(Fm) hydrogels formed at both acidic (4.9) and physiological (7.4) pH were more stable over several months and no degradation was observed, which is crucial for drug delivery and cell interaction studies. At basic pH, Fm-Dap(Fm) hydrogel was less stable and shows water expulsion in a couple of weeks.

3.2. Microscopic analysis

The morphology of the self-assembled structure of Fm-Dap(Fm) in the hydrogels was assessed by optical microscopy and scanning electron microscopy (SEM). It was observed that Fm-Dap(Fm) form nanofibrillar network structures upon gelation in all three pH conditions. The initial optical microscopic analysis of xerogels (air dried) derived from these hydrogels displayed a fibrillar morphology (Fig. S5). The corresponding SEM images exhibited nano-fibrillar structures (Fig. 2). Further, it is clear from the pictures that the width of the fibrils is increased with increasing pH. The statistical data analyses indicate that the Fm-Dap (Fm) widths of hydrogel fibrils vary from 150 to 250 nm, 250–300 nm and 250–600 nm at pH 4.9, 7.4, and 9.1, respectively (Fig. S6). The increase in width of fibers could be due to an increase in the lateral overlap of the lower order nanofibrils rather than individual fibrils. Such an increase in a diameter reduced the number of network points in the entanglement of the fibrillar network (*vide infra*). Nevertheless, at all three pHs, Fm-Dap(Fm) displayed nano-fibrillar network structures which are entangled to each other to form a three-dimensional network structure. These entangled fibrillar structures are most likely responsible for the immobilization of water molecules to form self-supporting Fm-Dap(Fm) hydrogels. The morphology of lyophilized hydrogels of Fm-Dap(Fm) was also analyzed to comprehend the effect of drying on the morphology of these hydrogels. The resulting SEM images exhibited a typical fibrillar structure for Fm-Dap(Fm) xerogel formed at different pH (Fig. S7). Both SEM results thus demonstrate that despite the method of water removal from the hydrogels, Fm-Dap(Fm) xerogel at different pH yielded a fibrillar morphology. AFM images of air-dried Fm-Dap(Fm) hydrogels at different pH were also recorded to further confirm the fibrillar morphology. From Fig. 3A-F, it is clear that self-assembled Fm-Dap(Fm) structure produces fibrils regardless of the pH condition. Further, the lateral overlap of nanofibrils was observed at neutral pH (Fig. 3D) which supports the SEM analysis. TEM images of air-dried Fm-Dap(Fm) hydrogels further confirms the formation of nanofibrils at different pH (Fig. S8).

3.3. Rheological analysis

Rheological studies were performed to understand the mechanical response and stability of the Fm-Dap(Fm) hydrogels. In rheological experiments, the shear storage modulus (G′) and loss modulus (G″) is examined as a function of strain, frequency, and time to gain critical properties of the gel [34]. The initial strain sweep results (Fig. 4A), which provides linear viscoelastic range (LVR), indicate that Fm-Dap (Fm) hydrogels formed at different pH exhibit a typical low molecular weight gel nature (G′ > G″) which breaks (G′ < G″) relatively at low strain (< 100%). Further, a characteristic feature of a viscoelastic gel, with G′ being higher than G″, was observed for all hydrogels up to the strain of 5%. The LVR results thus suggest that, at low strain amplitudes (linear regime), segments between the network points (i.e., fibrils) stretch elastically while the fibril segments stretch in a nonlinear fashion as the strain amplitude increases (nonlinear regime). Based on the LVR results, a strain of 0.5% was fixed for further rheological experiments.

Angular frequency sweep results (Fig. 4B) shows that G′ is dominating over G″ for the Fm-Dap(Fm) hydrogels and does not cross over in the frequency region of interest. At pH 4.9, both G′ and G″ almost remain the same with an increase in angular frequency, whereas, at other pHs, both moduli were weak functions of frequency. The nonlinear regime appears at relatively smaller strain amplitudes for gels formed at higher pH (7.4 and 9.1) could be due to the formation of more rigid fibers with fewer network points, which breaks more easily. The weak frequency dependence was supported by tan δ, which is drastically changed at higher frequencies for hydrogels except for hydrogel formed at 4.9, where it remains the same at ~ 0.09. It is also inferred that Fm-Dap(Fm) hydrogel at pH 4.9 has good tolerance to external forces compared to other pHs. Nonetheless, the observed weak frequency dependence of moduli is characteristic of a supramolecular gel derived from LMW gelators. It is noteworthy that storage modulus (G′) for Fm-Dap(Fm) hydrogel formed at pH 4.9 is the higher value at any given frequency compared to pH 7.4 and 9.1 (Fig. 4B). This result suggests that hydrogel obtained from pH 4.9 is more stable, which could be due to the favor of strong aromatic stacking interactions between fluorenyl moieties. The data at higher frequencies are not reported for hydrogel formed at pH 7.4 due to poor S/N ratio.

Thixotropic property (time-dependent shear thinning) of Fm-Dap (Fm) hydrogels was also analyzed. As can be seen from Fig. 5A, hydrogel (G′ > G″) formed at 4.9 transforms into a liquid (G′ < G″) upon applying a high stress (ON), but rapidly becomes a gel (G′ > G″) again when an applied stress was released (OFF). A similar result was observed for three cycles of ON-OFF stress. This result demonstrates that Fm-Dap(Fm) hydrogel at pH 4.9 has excellent thixotropic property, which is required for many applications. Similar behavior of moduli was observed for the other two pH hydrogels (Fig. 5B and C), indicating that Fm-Dap(Fm) has pH independent thixotropic nature. However, it should be noted that, at pH 4.9, the G′ gained almost 100% of an initial value upon release of strain at each cycle ends in the given relaxation time during low strain (OFF status). At pH 7.4 and 9.1, G′ gained a maximum of 88% and 66% at the end of the third cycle, respectively, and the percentage of recovery was found to be a cycle dependent. It is noteworthy that an average tan δ value of 0.09, 0.25, and 0.4 at pH 4.9, 7.4, and 9.1, respectively, were maintained upon release of strain (OFF), indicating that strength of the viscoelastic nature also maintained upon self-healing (Fig. S9). The thixotropic results thus suggest that hydrogel of Fm-Dap(Fm) has strong re-gelation (self-healing) ability at acidic pH, and the ability of re-gelation decreases with the increase of pH. It is noteworthy that the number of network points decreases with an increase in pH, as evidenced by SEM analysis.

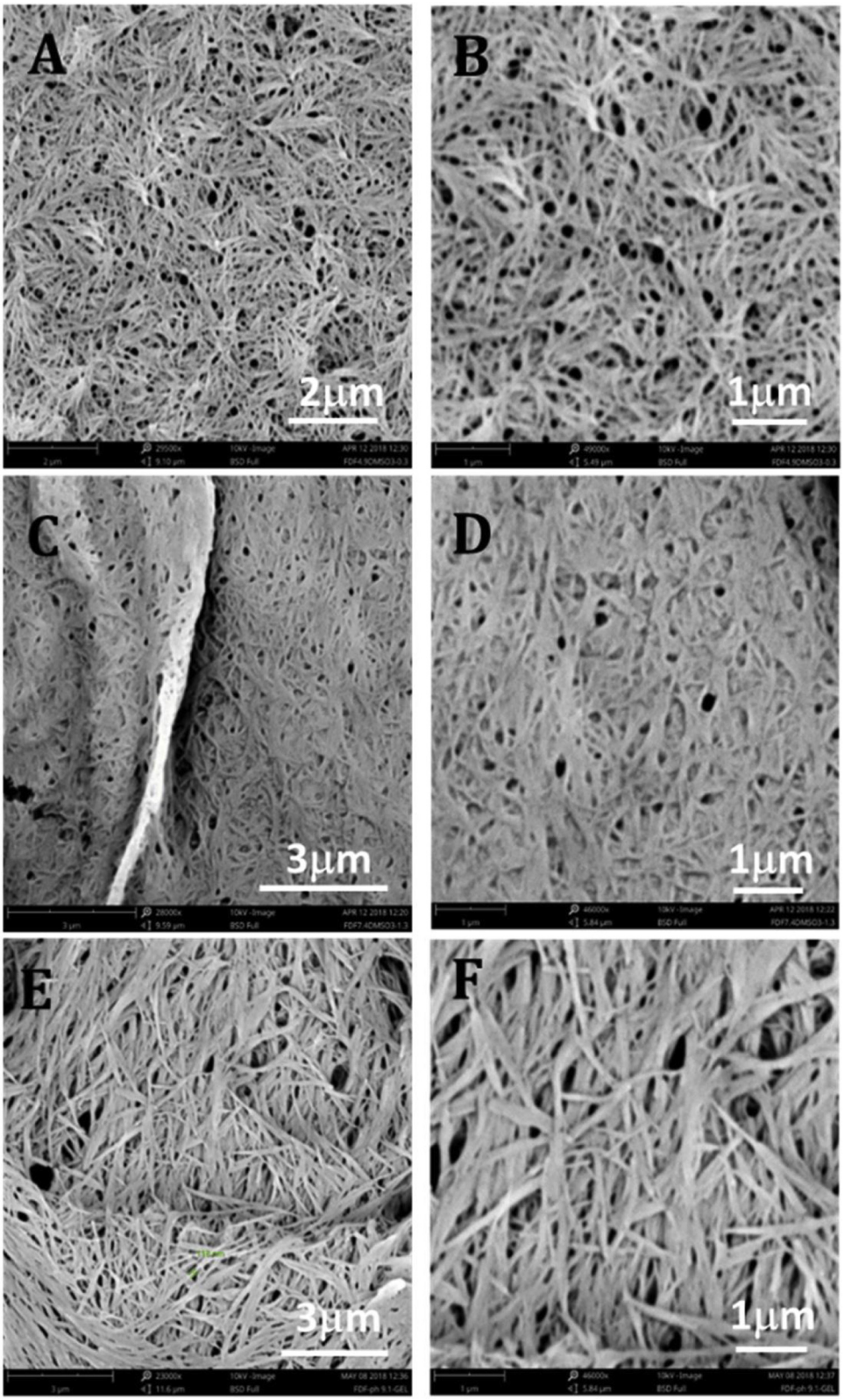

Fig. 2. SEM images of air-dried Fm-Dap(Fm) hydrogels at pH 4.9 (A and B), 7.4 (C and D), and 9.1 (E and F).

Therefore, the gels formed at low pH (4.9) exhibit higher moduli and better recovery than the gels formed at higher pH (7.4 and 9.1). A cartoon model illustrating the fibrillar network present in the Fm-Dap (Fm) hydrogel formed at different pH is presented in Fig. S10.

3.4. Thermal stability of hydrogels

The thermal stability of the Fm-Dap(Fm) hydrogels was studied by both rheology and conventional vial inversion method. From Fig. 5D, at pH 4.9, both the moduli were increased with increasing temperature and did not overlap at any temperature within the chosen range

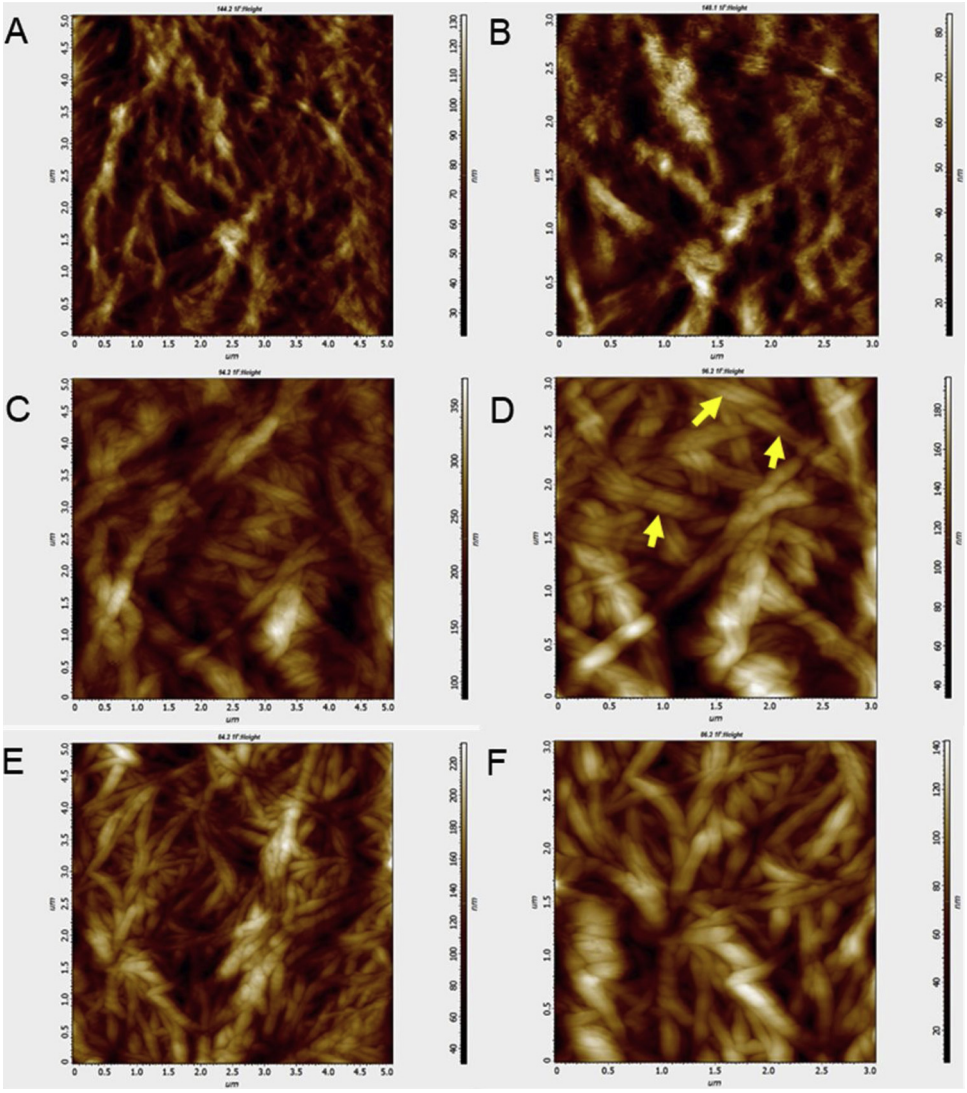

Fig. 3. AFM images of air-dried Fm-Dap(Fm) hydrogels at pH 4.9 (A and B), 7.4 (C and D), and 9.1 (E and F). The size of the AFM images are 5 × 5 μm (left panel) and 3 × 3 μm (right panel). Yellow arrow marks in Fig. D point the places where nanofibrils are laterally overlapped.

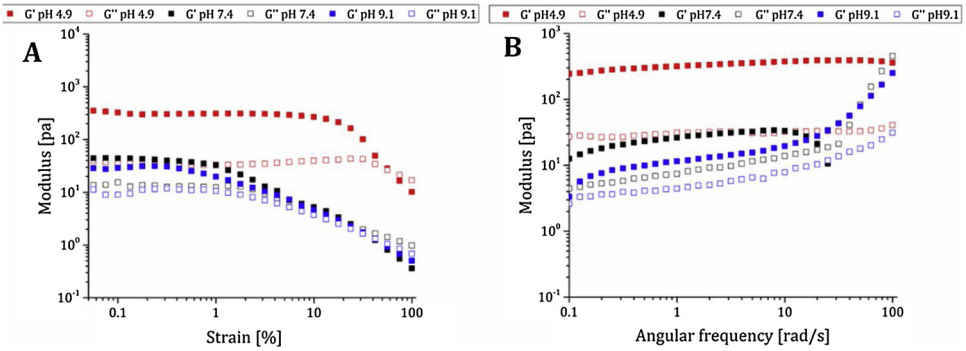

Fig. 4. Rheological measurements show strain sweep (A) and dynamic frequency sweep (B) for Fm-Dap(Fm) hydrogels formed at pH 4.9 (red), 7.4 (black) and 9.1 (blue).

(25–95 °C). This feature indicates that Fm-Dap(Fm) remains in the hydrogel form over the temperature range studied. The corresponding thermal stability test conducted by vial inversion method supports that Fm-Dap(Fm) hydrogel (pH 4.9) remain in the gel form up to 90 °C though it did not stick on the top of the vial upon inversion (Fig. S11). It was also observed that water was expelled from the gel with increasing temperature, which leads to the shrinkage of the hydrogel. After cooling to 25 °C, the magnitude of both storage (G′) and loss (G″) moduli increased drastically, especially G′ increased from 313 to 15,000 pa. An increase G′ value could be due to the hardening of the hydrogel because of water expel and also reducing the temperature, which arrests the molecular motion. The decrease of tan δ from 0.16 (90 °C) from 0.02 (25 °C) and an increase of storage modulus (G′) during cooling indicate that annealed hydrogel (pH 4.9) of Fm-Dap(Fm)

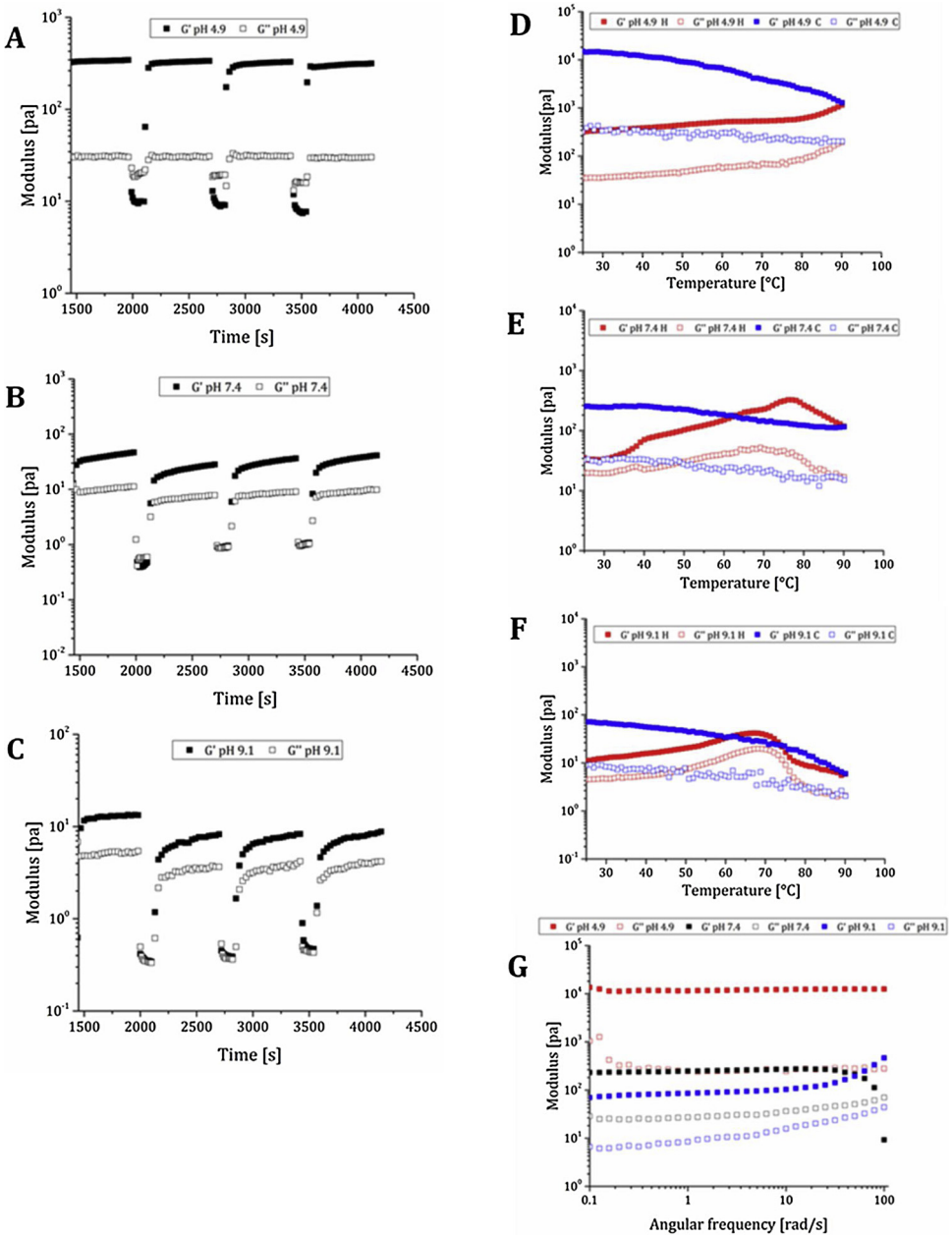

Fig. 5. Rheological measurements show continuous step-strain (thixotropy cycle) at a fixed frequency of (1 rad/s) for Fm-Dap(Fm) hydrogels formed at pH 4.9 (A), 7.4 (B) and 9.1 (C). Rheological measurements show continuous temperature sweep [both heating (Red trace) and cooling (blue trace)] for Fm-Dap(Fm) hydrogels formed at pH 4.9 (D), 7.4 (E) and 9.1 (F). (G) Dynamic frequency sweeps for Fm-Dap(Fm) hydrogels after annealing at different pHs.

has greater mechanical properties and superior elasticity than the corresponding normal hydrogel. Similar to pH 4.9, both storage (G′) and loss (G″) moduli was increased with increasing temperature and did not meet at any temperature between 25–90 °C for Fm-Dap(Fm) hydrogels formed at pH 7.4 and 9.1 (Fig. 5E and 5 F, respectively). Further, the magnitude of both moduli was increased upon cooling to 25 °C. The tan δ during heating and cooling remained below one which indicates that Fm-Dap(Fm) hydrogels retain viscoelastic gel nature at a wide range of temperature. But, the corresponding vial inversion test shows that hydrogels at pH 7.4 (Fig. S12) and 9.1 (Fig. S13) lost their self-supporting nature at elevated temperatures and broke physically at higher temperatures. However, the viscous nature of the solution was retained, which remains the same even after cooling to 25 °C and incubating for 16 h. This observation suggests that the self-supporting of hydrogels formed at 7.4 and 9.1 are thermally irreversible nature. The viscous nature of these Fm-Dap(Fm) hydrogels was supported by rheology data where G′ is greater than G″ during cooling. Nevertheless, all the gels show an increase in moduli upon heating and a hysteresis upon cooling, which could be attributed to the gradual loss of water from the network upon heating, which induces irreversible morphological changes leading to heating-enhanced stiffness. Upon cooling, new stronger network structures are formed that exhibit higher moduli as well as weak frequency dependence. Meanwhile, a dynamic frequency sweep was also performed for annealed hydrogels, and the same is presented in Fig. 5G. The results indicate that irrespective of pH, the characteristic of viscoelastic gel (G' > G″) was maintained over the frequency range for Fm-Dap(Fm) hydrogels.

3.5. Fluorescence and absorption spectroscopic analysis

Fluorescence spectroscopy is used to understand the intermolecular aromatic interactions between fluorenyl moieties [35] in the fibrils of

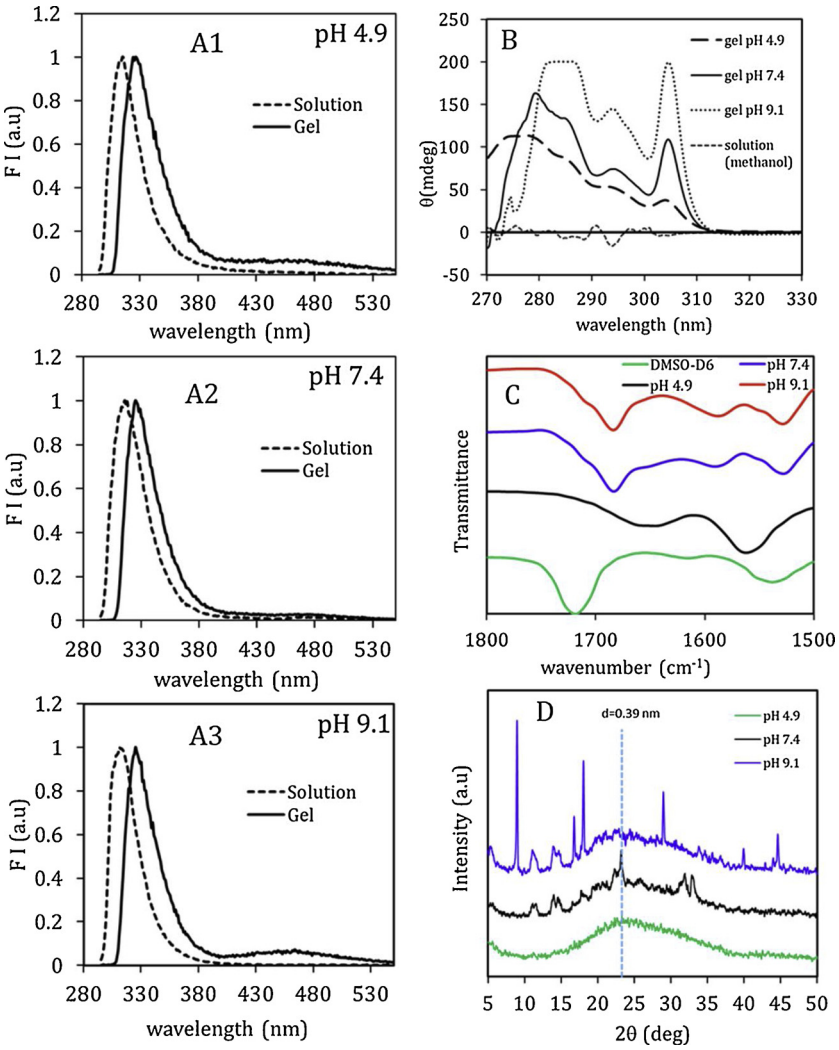

Fig. 6. (A1-A3) Fluorescence emission spectra of Fm-Dap(Fm) in solution and hydrogel form at different pH. (B) CD spectra of Fm-Dap(Fm) in solution (low concentration in methanol) and hydrogel at different pH. The flat-topped signal around 285 nm is due to high HT. (C) FTIR spectra of Fm-Dap(Fm) in solution (DMSO-d_6) and xerogel form of the hydrogel at different pH. (D) pXRD of xerogel of Fm-Dap(Fm) hydrogel formed at different pH.

Fm-Dap(Fm) hydrogels. Accordingly, steady-state fluorescence emission spectra of Fm-Dap(Fm) at low (solution) and high (hydrogel) concentrations in different pH were measured. As can be seen from Fig. 6, Fm-Dap(Fm) solution exhibited fluorescence wavelength emission maximum (λ_{max}) at 312 nm in pH 4.9 and 7.4 while the same has been slightly blue shifted to 308 nm in pH 9.1. Despite this difference, after hydrogelation at different pH, Fm-Dap(Fm) shows λ_{max} at 324 nm which is red shifted by 12–16 nm compared to the solution which is consistent with the previous report [32]. The current fluorescence results thus suggest that during hydrogelation, fluorenyl moieties participate in the aromatic-aromatic interactions through π-π stacking in an anti-parallel orientation. From Fig. 6(A1-A3), it is also noticed that Fm-Dap(Fm) hydrogels show an excimer band at 456 nm, which is indicative of multiple stacking of fluorenyl moieties. It is noteworthy that the excimer is more visible at acidic and basic pH, indicating that Fm-Dap(Fm) involved in extensive stacking in the hydrogels formed at these pHs. The stcking of fluorenyl moieties were also supported by absorption spectra where a characteristic λ_{max} around ~302 nm for fluorenyl moieties in hydrogel form was observed for all the hydrogels (Fig. S14). Notably, a slightly higher λ_{max} at acidic pH compared to other pHs indicates the extensive and strong stacking of fluorenyl moieties at acidic pH which supports the higher thermal stability and rheology property of Fm-Dap(Fm) hydrogel at pH 4.9. Nevertheless, fluorescence and absorption results established that the self-assembled structure of Fm-Dap(Fm) in the hydrogel form is stabilized by aromatic π-π stacking interaction between fluorenyl moieties.

3.6. CD analysis

It is well established that LMW gelators containing Fmoc- group are self-assemble with characteristic induced CD signals between 270 and 310 nm [36], which are attributed to a superhelical structure formed through Fmoc-Fmoc interactions. A specific peak at 306 nm is characteristic of displaced π-π stacking of fluorenyl moieties that occurs in the fibrillar assemblies. As can be seen from Fig. 6B, Fm-Dap(Fm) in methanol solution did not yield a CD while it produced strong CD signals in the hydrogels obtained from all the pH condition. The CD results thus support that self-assembled structure of Fm-Dap(Fm) in the hydrogels are stabilized by strong intermolecular aromatic interactions between fluorenyl moieties as evidenced by fluorescence analysis (*vide supra*). Further, the positive sign of the CD band at 306 nm indicates that the superhelical structures formed through π-π stacking of Fmoc moieties during the fibril formation are right handed twisted. The difference in the intensity of the band at 306 nm between pH 9.1 and 7.4 could be due to differential stacking interaction or higher order in the fibrillar structure. Since the MHGC at pH 4.9 is lower than other pHs, the low intensity is most likely due to the low concentration of Fm-Dap (Fm). Nonetheless, a combination of CD and fluorescence results

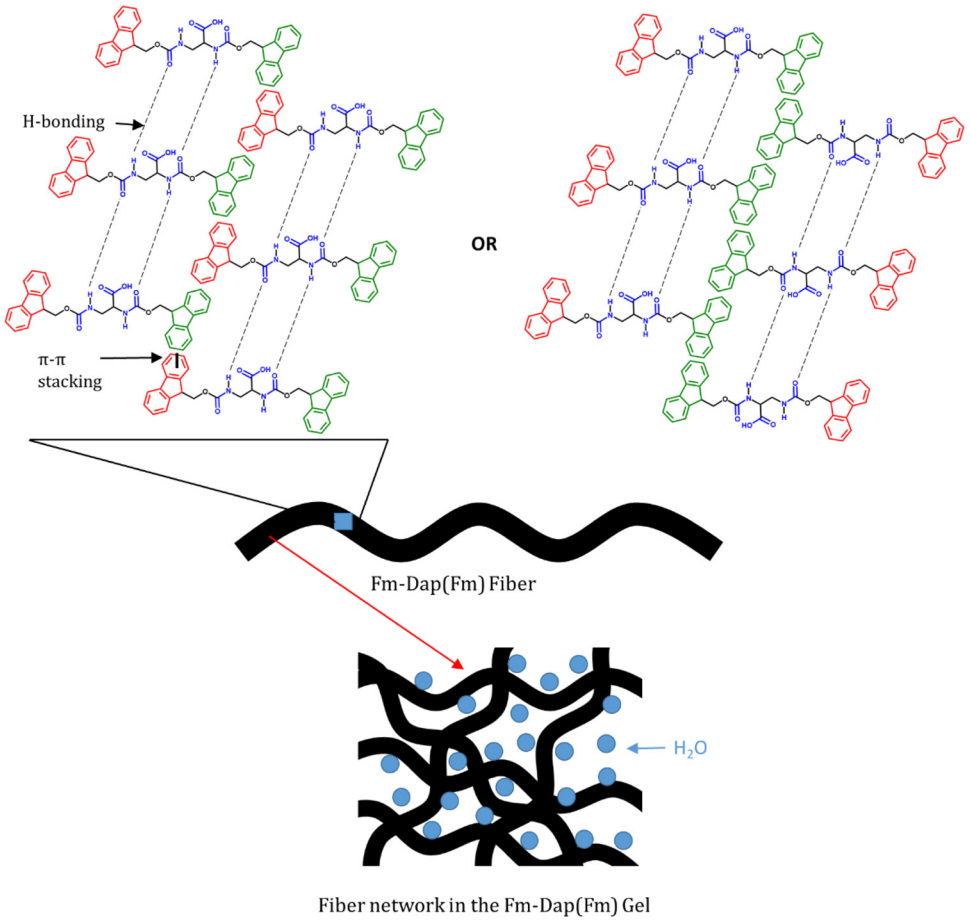

Fig. 7. Cartoon diagram shows the proposed self-assembly of Fm-Dap(Fm) in the hydrogels. Top images show the anti-parallel arrangement of Fm-Dap(Fm) molecules with head-to-tail (left) or tail-to-tail (right) orientation of fluorenyl moieties. Middle and bottom images show the fiber and the entanglement of fibers in the hydrogel, respectively.

demonstrate that the stacking of fluorenyl moieties is a critical step in the self-assembly process that leads to hydrogelation of Fm-Dap(Fm). A model has been proposed for Fm-Dap(Fm) self-assembled structure where fluorenyl moieties were stacked in an anti-parallel orientation (Fig. 7). This model also illustrates the possible hydrogen bonding pattern among carbamates, which is identified from the FTIR analysis (vide infra). Since Fm-Dap(Fm) is not a symmetric molecule, we proposed two possible models for the anti-parallel orientation of fluorenyl moieties though both of them were almost in a similar environment. In the first model, fluorenyl moieties are oriented in an anti-parallel orientation by head-to-tail while in the second model, fluorenyl moieties were oriented in the tail-to-tail direction (Fig. 7).

3.7. FT-IR analysis

FTIR is used to elucidate the role of hydrogen bonding in the stabilization of self-assembly in the hydrogel. In the present case, the FTIR spectrum of Fm-Dap(Fm) in monomer/solution form (dissolved in DMSO) shows a strong peak at 1714 cm^{-1} (Fig. 6C) which is attributed to free carbamate group (carbonyl associated with Fmoc moiety). As described earlier [4], the carbonyl group in a carboxylic acid (−COOH) of conjugated amino acid appears between 1740 and 1700 cm^{-1}, and hence it is presumed that C═O stretching vibration of −COOH in Fm-Dap(Fm) is overlapped at 1714 cm^{-1}. In the xerogel of Fm-Dap(Fm) hydrogels, the stretching frequency of carbamate at 1714 cm^{-1} is split into two, and they are shifted to a lower frequency. The larger shift to 1683 cm^{-1} (strong band) at pH 9.1 and 7.4, compared to solution state, indicates that Fmoc carbonyl groups are involved in the hydrogen bonding network. Although two Fmoc carbonyl groups are present in the Fm-Dap(Fm) molecule, the appearance of the single strong band at 1683 cm^{-1} suggests that both the carbonyl groups are overlapped and involved in similar hydrogen bonding network. At pH 4.9, the stretching frequency of Fmoc carbonyl groups in Fm-Dap(Fm) hydrogel appears as a doublet at 1660 and 1645 cm^{-1} which could be attributed to two Fmoc carbonyl groups. The larger shift of Fmoc carbonyl groups compared to hydrogels formed at pH 7.4 and 9.1 suggest that hydrogen bonding present in the Fm-Dap(Fm) hydrogel at acidic pH is stronger than the other two pHs. This interpretation is supported by thermal melting studies where hydrogel formed at acidic pH exhibited higher thermal stability compared to other pHs. Although not clear at acidic pH, the appearance of weak shoulder band at 1706 cm^{-1} for Fm-Dap (Fm) hydrogels at pH 7.4 and 9.1 suggests that carbonyl group associated with −COOH is also participating in the hydrogen bonding network. The formation of hydrogen bonding between carbonyl and N−H groups is supported by N−H region where the characteristic band is observed at 3373-3357 cm^{-1} for hydrogen-bonded amide N−H groups [37] (Fig. S15). The involvement of hydrogen bonds in the stabilization of fibrils supports the proposed model for the self-assembled structure of Fm-Dap(Fm) in its hydrogel form (Fig. 7).

3.8. NMR analysis

^{1}H NMR spectra of Fm-Dap(Fm) hydrogels provide the involvement of various species of Fm-Dap(Fm) in its self-assembled structure at atomic level. Fig. S16 shows an absence of proton signals in the hydrogel form (25 °C) of Fm-Dap(Fm) at different pH. The complete broadening out of proton signals indicates that the motional freedom of both aromatic fluorenyl protons and aliphatic methylene protons are significantly reduced due to hydrogel form at all pHs. At high temperature (65 °C), the appearance of broad signals in the aromatic fluorenyl proton region and weak signals in the aliphatic methylene proton region at pH 9.1 suggests the partial breaking of hydrogel which

produces some amount of free Fm-Dap(Fm) molecules. A similar result was observed for Fm-Dap(Fm) hydrogels at pH 7.4 and 4.9, but with significantly reduced signal intensity compared to pH 9.1 (Fig. S16). However it should be noted that none of the hydrogels showed sharp signals at higher temperature which suggests that Fm-Dap(Fm) exists in the gel/viscous form at higher temperature which is consistent with rheology. The temperature-dependent ^{1}H NMR results thus confirm that aromatic interactions between fluorenyl species are the primary force, which stabilizes the self-assembled structure of Fm-Dap(Fm), while hydrophobic interaction between methylene groups provides necessary support for the stability of the fibrils. Indirectly, the latter result supports the formation of intermolecular hydrogen bonds between carbamate groups, which can arrest the motional freedom of methylene protons as they are close to them (Fig. 7).

3.9. pXRD and polarized optical microscopic analysis

X-ray diffractions (XRD) data offers crucial evidence of the molecular packing in the well-defined self-assembled systems. Hence, power XRD (pXRD) pattern was recorded for the air-dried hydrogels and found a weak broad peak for hydrogel formed at pH 4.9 and some weak peaks for the hydrogel formed at pH 7.4 (Fig. 6D). At pH 9.1, some sharp peaks were observed in addition to a broad peak. In general, the weak broad peak is indicative of highly fibrous nature while the sharp peaks suggest the crystalline nature. Consequently, the weak broad peak of Fm-(Dap)Fm hydrogel formed at pH 4.9 indicates that the fibrillar structure possesses a high fibrous character which decreases with the increase of pH as evidenced from increases sharp peaks at basic pH. Despite the pH, all pXRD data showed a peak centered at ~ 0.39 nm (Fig. 6D), which is the characteristic d-spacing value of aromatic π-π stacking interactions. This result suggests that molecular packing of Fm-Dap(Fm) during self-assembly in different aqueous pH solutions mostly likely to follow a similar mechanism which results in common nanofibrillar structures.

3.10. Enhanced cellular adhesion and coating by Fm-Dap(Fm) hydrogel

Screening, selection, and preparing the novel biocompatible substrate for mammalian cell culture is paramount importance in recent years. In this context, we expected that the newly developed Fm-Dap (Fm) hydrogel, which as unique non-proteinogenic amino acid (Dap), might act as a substrate to facilitate mammalian cell culture. The MTT assay of human fibroblasts (3T3) cells revealed that the 0.25 mM of Fm-Dap(Fm) hydrogel coating on the plate showed remarkable cellular viability over three days due to an efficient cell adhesion followed by cell proliferation (Fig. S17). Further increasing the concentration higher than 0.25 mM clearly shows the lesser cell viability, which could be due to poor cell adhesion resulted in poor cell viability. Extending the incubation period of 3T3 cells confirm the toxicity resulted in reduced cell adhesion at high concentrations. The staining data of flurorescence images support the MTT assay that Fm-Dap(Fm) incorporated hydrogels showed efficient cell viability by appearing a large number of viable cells at 0.25 mM (Fig. 8) and increasing concentration resulted with a mixed population of live (green) and dead (red) cells.

3.11. Effect of Fm-Dap(Fm) in gene regulation and on Cell Proliferation

To understand the cell proliferation, we selected the nuclear protein Ki-67 and proliferating cell nuclear antigen (PCNA) as markers which are actively involved in replication as well as in cell cycle. The flow cytometry data revealed that the cells were grown on Fm-Dap(Fm) hydrogel showed a significant increase of Ki-67 marker (99.9%) (Fig. S18E) which is considerably higher than the control cells (68.7%) (Fig. S18B). Followed by cell proliferation analysis using PCNA supports the significant differences only among the cell grown on the Fm-Dap(Fm) hydrogel (99.9%) (Fig. S18D) compared to the control cells (58.2%) (Fig. S18C). It was evident that the Ki and PCNA expression percentages were higher in the Fm-Dap(Fm) hydrogel grown cells (Fig. S18). The data demonstrate that Fm-Dap(Fm) up-regulate cell proliferating genes directly or indirectly and induce proliferation and migrating responsible signaling pathway in the cells. To explore the molecular mechanism, the relative gene expression of cell grown proliferating markers of cell grown on Fm-Dap(Fm) hydrogel was quantified. After 48 h incubation, the mRNA expression of PCNA and Ki-67 was up-regulated by Fm-Dap(Fm) hydrogel at the concentration of 0.25 mM. There were a 9.8-fold increase and 1.25-fold increase in the expression of PCNA and Ki-67, respectively (Fig. S19). The synthesis of PCNA and Ki-67 were low in quiescent cells and increases during the S phase of the cell cycle. The overall cell viability analyses support that Fm-Dap(Fm) hydrogel could be an ideal biologically compatible substratum for cell therapies and regenerative medicine.

3.12. Proteolytic stability of Fm-Dap(Fm) hydrogel

The Fm-Dap(Fm) gelator has non-protein amino acid (Dap) and lacks a typical amide bond in the chemical structure. Therefore, it is expected that this gelator shows resistance towards proteolysis. To test this hypothesis, a proteolytic stability study was conducted by incubating Fm-Dap(Fm) hydrogel without (control) and with proteinase K (test) in phosphate buffer for 48 h. The degradation was monitored by reading absorbance at 303 nm (associated with fluorenyl moiety) and also by visual inspection. No significant change in the absorbance data between test and control after 48 h incubation confirms that Fm-Dap (Fm) hydrogel is resistant towards proteolysis. The corresponding digital images of Fm-Dap(Fm) hydrogel in the presence and absence of proteinase K (Fig. S20) remain same after 48 h incubation which further confirms that Fm-Dap(Fm) hydrogel has resistant to proteolysis. The results thus suggest that Fm-Dap(Fm) hydrogel could be an ideal biomaterial in antibiotic-resistant microorganism pathogenesis.

3.13. Drug release studies

Since the MTT assay results revealed not only cell viability but also cell proliferation, Fm-Dap(Fm) hydrogel formed at physiological pH (7.4) was explored for the encapsulation and controlled drug delivery. Accordingly, Fm-Dap(Fm) hydrogel was induced by the buffer containing vitamin $B_{12,}$ and the result shows the formation of a stable hydrogel. The stability of hydrogel suggests that drug molecules can be encapsulated in the Fm-Dap(Fm) hydrogel matrix without disturbing the hydrogelation process. The release properties of encapsulated vitamin B_{12} from the co-assembled hydrogel was monitored at 525 nm. It is clear that vitamin loaded hydrogel shows a release over 24 h with a maximum discharge of ~ 50% after 7 h, then reaching a plateau (Fig. S21). The release of the drug was also confirmed visually by the color change of the added buffer solution on the top of the hydrogel as a function of time (image not is shown). It also observed that the addition of fresh buffer on the top hydrogel by replacing the old buffer yielded further release. Nevertheless, the release studies revealed the Fm-Dap (Fm) hydrogel formed at physiological pH 7.4 could deliver the drugs.

4. Conclusions

Herein, we have successfully developed a new Fm-Dap(Fm) LMW hydrogel material containing non-proteinogenic amino acid namely 2,3-diaminopropionic acid (Dap), a key precursor in the synthesis of many antibiotics namely viomycin and capreomycin. Di-Fmoc functionalization of Dap induced hydrogelation with pH stimulus response. Fm-Dap(Fm) exhibited hydrogelation with a broad range from pH 4.9 to 9.1. Both temperature and rheological studies indicated that both thermal and mechanical stability of Fm-Dap(Fm) hydrogel depends on the pH and Fm-Dap(Fm) has higher thermal stability and high mechanical stability at acidic pH compared to neutral and basic pH. All

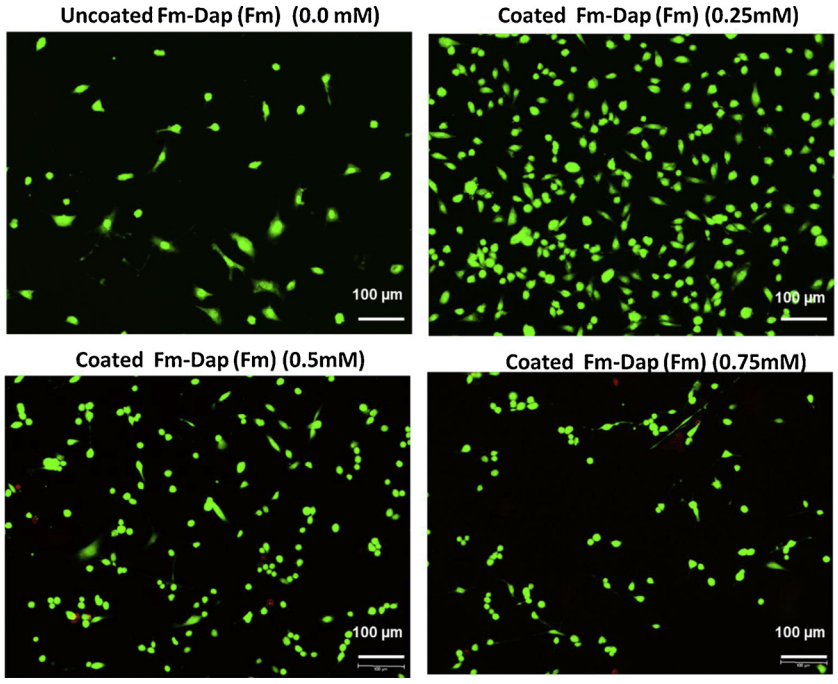

Fig. 8. Fluorescence images show the 3T3 cells treated with Fm-Dap(Fm) hydrogel (pH 7.4) at varying concentrations of 0.25, 0.5, 0.75 mM. The cells were stained with calcein AM/Ethidium bromide. Scale bar represents 100 µm.

Fm-Dap(Fm) gels comprise of fibrils that entangle to form a three-dimensional network structure wherein each fibril is intrinsically stabilized by intermolecular aromatic π-π stacking and H-bonding interactions. The proteolytic study indicated that Fm-Dap(Fm) hydrogel is resistant against proteolysis. Further, the current study demonstrated that the newly development non-proteinogenic amino acid containing Fm-Dap(Fm) gelator has biocompatibility with enhanced cell proliferation which is crucial in cell culture and tissue engineering if one considers supramolecular hydrogel as the substrate material. We thus believe that the development of non-proteinogenic amino acid-based supramolecular hydrogel provides a new biomaterial which can be utilized for various biological applications, especially in drug delivery and tissue engineering. We also strongly believe that the current findings offer a lead to construct or design new synthetic non-proteinogenic amino acid (Dap)-based LMW organic gelators for several potential applications.

Declaration of interests

The authors declare that they have no known competing financial interests or personal relationships that could have appeared to influence the work reported in this paper.

Supporting information

Supporting information includes Figs. S1-S21 and also the detailed experimental procedures on cell viability and proliferation studies, flow cytometry studies, and gene expression studies using real time-PCR.

Acknowledgements

The financial support by the Council of Scientific and Industrial Research (CSIR) under Major Laboratory Project (MLP-27) is greatly acknowledged. The CSIR-CLRI communication number is CLRI-MLP-27/1320. We thank the Director, CSIR-CLRI, for his permission to publish this work. Authors would like to thank Mr. M Muthukrishnan, Senior Technical Officer, Advanced Biomaterial Laboratory, CSIR-CLRI, for his help in SEM and TEM measurements. Mr. Samala Murali Mohan Reddy, Senior Research Fellow, CSIR-CLRI, is acknowledged for his initial technical help. A. P. D. thanks the Department of Science and Technology, India for financial support. Authors also thank Mr R Ravikanth Reddy, Research Scholar, CSIR-CLRI, for his help in NMR experiments.

Appendix A. Supplementary data

Supplementary material related to this article can be found, in the online version, at doi:https://doi.org/10.1016/j.colsurfb.2019.110581.

References

[1] T. Liebmann, S. Rydholm, V. Akpe, H. Brismar, Self-assembling Fmoc dipeptide hydrogel for in situ 3D cell culturing, BMC Biotechnol. 7 (2007) 88.
[2] J. Ryu, S.-W. Kim, K. Kang, C.B. Park, Mineralization of self-assembled peptide nanofibers for rechargeable Lithium ion batteries, Adv Mater 22 (2010) 5537–5541.
[3] M. Ikeda, T. Tanida, T. Yoshii, K. Kurotani, S. Onogi, K. Urayama, I. Hamachi, Installing logic-gate responses to a variety of biological substances in supramolecular hydrogel-enzyme hybrids, Nat. Chem. 6 (2014) 511–518.
[4] S.M.M. Reddy, G. Shanmugam, N. Duraipandy, M.S. Kiran, A.B. Mandal, An additional fluorenylmethoxycarbonyl (Fmoc) moiety in di-Fmoc-functionalized l-lysine induces pH-controlled ambidextrous gelation with significant advantages, Soft Matter 11 (2015) 8126–8140.
[5] S. Ray, A.K. Das, A. Banerjee, pH-responsive, Bolaamphiphile-Based Smart Metallo-Hydrogels as potential dye-adsorbing agents, water purifier, and vitamin B12 carrier, Chem. Mater. 19 (2007) 1633–1639.
[6] B.O. Okesola, D.K. Smith, Applying low-molecular weight supramolecular gelators in an environmental setting – self-assembled gels as smart materials for pollutant removal, Chem. Soc. Rev. 45 (2016) 4226–4251.
[7] W. Zhang, X. Zhou, T. Liu, D. Ma, W. Xue, Supramolecular hydrogels co-loaded with camptothecin and doxorubicin for sustainedly synergistic tumor therapy, J. Mater. Chem. B Mater. Biol. Med. 3 (2015) 2127–2136.
[8] F. Song, L.-M. Zhang, J.-F. Shi, N.-N. Li, C. Yang, L. Yan, Using hydrophilic polysaccharide to modify supramolecular hydrogel from a low-molecular-mass gelator, Mater. Sci. Eng. C 30 (2010) 804–811.
[9] Y. Song, J. Gao, X. Xu, H. Zhao, R. Xue, J. Zhou, W. Hong, H. Qiu, Fabrication of thermal sensitive folic acid based supramolecular hybrid gels for injectable drug release gels, Mater. Sci. Eng. C 75 (2017) 706–713.
[10] Y.-M. Zhang, J.-X. He, W. Zhu, Y.-F. Li, H. Fang, H. Yao, T.-B. Wei, Q. Lin, Novel pillar[5]arene-based supramolecular organic framework gel for ultrasensitive response Fe3+ and F− in water, Mater. Sci. Eng. C 100 (2019) 62–69.
[11] D. Khatua, R. Maiti, J. Dey, A supramolecular hydrogel that responds to biologically relevant stimuli, Chem. Commun. (Camb.) (2006) 4903–4905.
[12] S. Matsumoto, S. Yamaguchi, S. Ueno, H. Komatsu, M. Ikeda, K. Ishizuka, Y. Iko,

K.V. Tabata, H. Aoki, S. Ito, H. Noji, I. Hamachi, Photo gel-sol/sol-gel transition and its patterning of a supramolecular hydrogel as stimuli-responsive biomaterials, Chemistry 14 (2008) 3977–3986.
[13] C. Wu, R. Li, Y. Yin, J. Wang, L. Zhang, W. Zhong, Redox-responsive supramolecular hydrogel based on 10-hydroxy camptothecin-peptide covalent conjugates with high loading capacity for drug delivery, Mater. Sci. Eng. C 76 (2017) 196–202.
[14] A. Vashist, A. Vashist, Y.K. Gupta, S. Ahmad, Recent advances in hydrogel based drug delivery systems for the human body, J. Mater. Chem. B Mater. Biol. Med. 2 (2014) 147–166.
[15] A.L. Rodriguez, T.Y. Wang, K.F. Bruggeman, C.C. Horgan, R. Li, R.J. Williams, C.L. Parish, D.R. Nisbet, In vivo assessment of grafted cortical neural progenitor cells and host response to functionalized self-assembling peptide hydrogels and the implications for tissue repair, J. Mater. Chem. B Mater. Biol. Med. 2 (2014) 7771–7778.
[16] F. Xu, J. Liu, J. Tian, L. Gao, X. Cheng, Y. Pan, Z. Sun, X. Li, Supramolecular self-assemblies with nanoscale RGD clusters promote cell growth and intracellular drug delivery, ACS Appl. Mater. Interfaces 8 (2016) 29906–29914.
[17] A. Mahler, M. Reches, M. Rechter, S. Cohen, E. Gazit, Rigid, self-assembled hydrogel composed of a modified aromatic dipeptide, Adv Mater 18 (2006) 1365–1370.
[18] Z. Yang, G. Liang, M. Ma, Y. Gao, B. Xu, Conjugates of naphthalene and dipeptides produce molecular hydrogelators with high efficiency of hydrogelation and super-helical nanofibers, J. Mater. Chem. 17 (2007) 850–854.
[19] F.-Y. Wu, S.-M. Hsu, H. Cheng, L.-H. Hsu, H.-C. Lin, The effect of fluorine on supramolecular hydrogelation of 4-fluorobenzyl-capped diphenylalanine, New J. Chem. 39 (2015) 4240–4243.
[20] W.C. Chan, P.D. White, Fmoc solid phase peptide synthesis, A Practical Approach, Oxford University Press, Oxford, UK, 2000.
[21] R. Vegners, I. Shestakova, I. Kalvinsh, R.M. Ezzell, P.A. Janmey, Use of a gel-forming dipeptide derivative as a carrier for antigen presentation, J. Pept. Sci. 1 (1995) 371–378.
[22] S. Mukherjee, T. Kar, P.K. Das, Pyrene-based fluorescent supramolecular hydrogel: scaffold for energy transfer, Chem. Asian J. 9 (2014) 2798–2805.
[23] Y. Shi, J. Wang, H. Wang, Y. Hu, X. Chen, Z. Yang, Glutathione-triggered formation of a Fmoc-protected short peptide-based supramolecular hydrogel, PLoS One 9 (2014) e106968.
[24] K. Basu, A. Baral, S. Basak, A. Dehsorkhi, J. Nanda, D. Bhunia, S. Ghosh, V. Castelletto, I.W. Hamley, A. Banerjee, Peptide based hydrogels for cancer drug release: modulation of stiffness, drug release and proteolytic stability of hydrogels by incorporating d-amino acid residue(s), Chem. Commun. (Camb.) 52 (2016) 5045–5048.
[25] G. Cheng, V. Castelletto, R.R. Jones, C.J. Connon, I.W. Hamley, Hydrogelation of self-assembling RGD-based peptides, Soft Matter 7 (2011) 1326–1333.
[26] T. Pospišil, L. Ferhatović Hamzić, L. Brkić Ahmed, M. Lovrić, S. Gajović, L. Frkanec, Synthesis, characterization and in vitro biocompatibility assessment of a novel tripeptide hydrogelator, as a promising scaffold for tissue engineering applications, Biomater. Sci. 4 (2016) 1412–1416.
[27] P. Kasperkiewicz, D. Gajda Anna, M. Drąg, Current and prospective applications of non-proteinogenic amino acids in profiling of proteases substrate specificity, Biol. Chem. 393 (2012) 843.
[28] M.G. Thomas, Y.A. Chan, S.G. Ozanick, Deciphering tuberactinomycin biosynthesis: isolation, sequencing, and annotation of the viomycin biosynthetic gene cluster, Antimicrob. Agents Chemother. 47 (2003) 2823–2830.
[29] E.A. Felnagle, M.R. Rondon, A.D. Berti, H.A. Crosby, M.G. Thomas, Identification of the biosynthetic gene cluster and an additional gene for resistance to the anti-tuberculosis drug capreomycin, Appl Env Microbiol 73 (2007) 4162–4170.
[30] N. Audic, G. Potier, N.A. Sasaki, New 2,3-diaminopropionic acid inhibitors of AGE and ALE formation, Org. Biomol. Chem. 11 (2013) 773–780.
[31] Y. Lan, B. Langlet-Bertin, V. Abbate, L.S. Vermeer, X. Kong, K.E. Sullivan, C. Leborgne, D. Scherman, R.C. Hider, A.F. Drake, S.S. Bansal, A. Kichler, A.J. Mason, Synthesis of L-2,3-Diaminopropionic acid, a siderophore and antibiotic precursor, Cell 21 (2014) 379–388.
[32] A.M. Smith, R.J. Williams, C. Tang, P. Coppo, R.F. Collins, M.L. Turner, A. Saiani, R.V. Ulijn, Fmoc-diphenylalanine self assembles to a hydrogel via a novel architecture based on π–π interlocked β-Sheets, Adv Mater 20 (2008) 37–41.
[33] S.M.M. Reddy, P. Dorishetty, G. Augustine, A.P. Deshpande, N. Ayyadurai, G. Shanmugam, A low-molecular-Weight gelator composed of pyrene and fluorene moieties for effective charge transfer in supramolecular ambidextrous gel, Langmuir 33 (2017) 13504–13514.
[34] C. Yan, D.J. Pochan, Rheological properties of peptide-based hydrogels for biomedical and other applications, Chem. Soc. Rev. 39 (2010) 3528–3540.
[35] S. Fleming, S. Debnath, P.W. Frederix, T. Tuttle, R.V. Ulijn, Aromatic peptide amphiphiles: significance of the Fmoc moiety, Chem. Commun. (Camb.) 49 (2013) 10587–10589.
[36] D.M. Ryan, T.M. Doran, B.L. Nilsson, Complementary pi-pi interactions induce multicomponent coassembly into functional fibrils, Langmuir 27 (2011) 11145–11156.
[37] M. Suzuki, M. Yumoto, H. Shirai, K. Hanabusa, Supramolecular gels formed by amphiphilic low-molecular-Weight gelators of Nα,Nε-Diacyl-L-Lysine derivatives, Chem. Eur. J. 14 (2008) 2133–2144.